The hydrodynamic interaction of two slowly evaporating spheres

Hasan N. Oguz and Andrea Prosperetti
Department of Mechanical Engineering, The Johns Hopkins University, Baltimore, Maryland 21218
Dario Antonelli
Industrie Face Standard, Viale Bodio 33, 20158 Milano, Italy

(Received 8 March 1989; accepted 16 June 1989)

The Stokes flow induced by the slow evaporation or condensation of two spheres is studied. The phase-change velocity is prescribed and uniform over the surfaces of the spheres. Exact expressions are obtained for the streamfunction and the drag forces. Simpler expressions applicable to a variety of limit cases (distant spheres, a source and a sphere, and a sphere and a plane) are presented. When only one sphere is evaporating, depending on the distance from the other sphere, the flow may exhibit a variety of interesting behaviors such as smooth-boundary separation, closed recirculating eddies, and infinite open eddies.

I. INTRODUCTION

The hydrodynamic interaction between two spheres in low-Reynolds-number flow is a classic problem to which many papers have been devoted.[1–6] The novel aspect of this problem, which is investigated here, is the effect of the evaporation or condensation of one or both spheres.

Specifically, we consider the steady flow that is established as a result of a prescribed constant and uniform normal velocity on the surface of the spheres and calculate the streamfunction and the forces that each sphere exerts on itself and on the other sphere as a consequence of this phase-change process. Some cases previously considered in the literature, such as a source in the presence of a sphere[7–9] and a sphere moving toward a plane wall,[10,11] are contained in our results. Since the flow is studied in the Stokes approximation, the problem is linear and the drag resulting from other external flow fields can be added to our expressions.

It will be clear from the results to be discussed below, which are to some extent unexpected, that the present problem possesses an intrinsic fluid mechanic interest. However, our original motivation in studying it has been its bearing on multiphase phenomena. An example may be found in a cloud of particles (e.g., smog or other atmospheric pollutants), which undergo sublimation or absorb gases. Small droplets in such diverse situations as the nucleation stage of condensation (e.g., rain formation), mist flow near the exit of a boiling channel at high heat fluxes, or cooling towers, furnish other examples. In all these situations the modeling at small, but finite, volume fraction of the disperse phase requires a knowledge of the pairwise interparticle forces. For instance, Batchelor[12] has shown how the sedimentation velocity of a cloud of spheres depends on such forces to first order in the volume fraction. Similarly, in the modeling of multiphase processes by averaged equations, the phasic momentum equations contain source terms, which account for the interphase forces. Therefore, whatever the approach, a significant role is played by these forces and the way in which they are affected by phase change is of interest. In the actual physical process the reciprocal effect, namely, the influence of the hydrodynamic interaction of the particles on the phase-change process, is also important. We do not address this problem here, but concern ourselves exclusively with the fundamental understanding of the fluid mechanic aspects of the situation described. This circumstance enables us to make several simplifying assumptions.

By prescribing a uniform evaporation velocity at the surface of the particles we uncouple the problem from its heat transfer aspects. This approximation will be acceptable when the latent heat is transported to the surface mainly from the interior of the sphere, with only a small fraction coming from the vapor side. Examples are sublimation or phase change at low superheats or subcoolings in the absence of boundaries. For a nonuniform phase-change rate, the normal velocity at the surface of the sphere must be expanded in a series of suitable eigenfunctions and our results will only apply to the first term in such an expansion. Nevertheless, when the drops are not too close, and in the absence of extreme anisotropies, the salient features of the process can be expected to be captured by our simplified approach.

The particles are taken to be spherical, which is reasonable for small fluid drops because of surface tension, but is at best an idealization for solid particles. The neglect of any internal circulation in the case of droplets is justified on the basis of the small viscosity of the vapor phase relative to that of the liquid.

The Reynolds number based on the evaporation velocity may be estimated by means of the following heat flux balance at the surface of the evaporating particle:

$$k_p(\Delta T/R) \simeq L\rho_v V, \tag{1}$$

where k_p is the particle's thermal conductivity, ΔT is its superheat, ρ_v the vapor density, and L the latent heat. From this relation we find

$$\mathrm{Re} \equiv \rho_v VR/\mu_v = k_p\,\Delta T/L\mu_v.$$

With the physical properties of water at 100 °C, this gives $\mathrm{Re} \sim 0.024\,\Delta T$, which is a small number for superheats realizable in practice. This circumstance justifies the usual assumptions of Stokes flow. Furthermore, in a slow flow, inertia forces are unimportant and therefore the distance between the spheres enters the problem only as a parameter even if, as a consequence of the mutual interaction forces, this distance were to vary with time.

To examine the assumption of steady evaporation, consider the typical case of particles subject to a slowly falling

 0899-8213/89/101656-10$01.90

ambient pressure, as would happen, for instance, in the case of a mist falling down a conduit. For our results to be applicable, the inverse time scale for this pressure drop, $|(1/p)dp/dt|$, where the derivative is taken following the particles, must be smaller than the inverse of the diffusion time in the particles t_d, given by

$$t_d = R^2/\chi_p, \tag{2}$$

where χ_p is the particles' thermal diffusivity. Typical pressure gradients dp/dz in pipes in the annular flow regime are of the order of a few kilo-Newtons per cubic meter, with corresponding flow velocities U of a few tens of meters per second. With $p \sim 10^5$ Pa, we then find $(p/U)/(dp/dz)$ of the order of a few seconds. A water drop at 100 °C has a comparable diffusion time for a radius in the millimeter range.

There are several methods for the solution of the Stokes flow equations in the presence of two spherical boundaries. Here, as has already been done in closely related problems,[4,10,11,13–18] we use bispherical coordinates. Although straightforward in nature, the solution technique requires a special treatment of the source term, a fact that does not seem to have always been correctly recognized in the past.[19]

In the next section we state the mathematical problem and derive its analytical solution. Some limit cases are studied in Sec. III. A detailed examination of the flow field is given in Sec. IV and the results for the interparticle forces are presented in Sec. V.

II. ANALYSIS

We consider two spherical particles surrounded by an incompressible viscous fluid in an otherwise unbounded region (Fig. 1). The normal velocity $V_j, j = 1,2$, of the fluid at the surface of the jth particle is uniform and given. Because of the neglect of any internal circulation, the tangential velocity at the particle surface vanishes. The problem is governed by the usual continuity and momentum equations in the Stokes approximation

$$\nabla \cdot \mathbf{u} = 0, \tag{3}$$

$$\nabla p = \mu \nabla^2 \mathbf{u}, \tag{4}$$

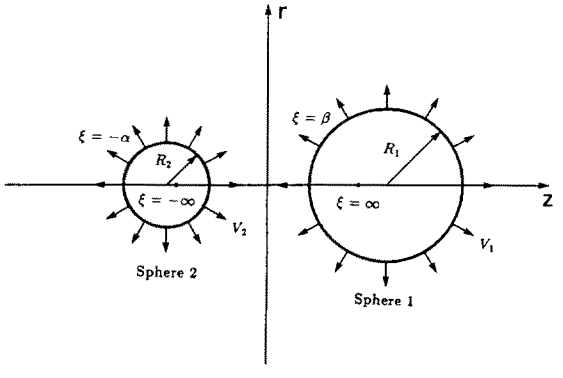

FIG. 1. Schematic of the two evaporating spheres of radii R_1 and R_2. In the bipolar coordinate sytem they are represented by $\xi = \beta$ and $\xi = -\alpha$, respectively. The evaporation rates (i.e., the normal velocities at the spheres' surfaces) are uniform and equal to V_1 and V_2, respectively.

where $\mathbf{u}$ is the velocity field, p is the pressure, and μ is the viscosity of the vapor.

The problem possesses an axis of symmetry in the line joining the centers of the spheres. Cylindrical coordinates (r,z), referred to this axis, are given in terms of the bipolar coordinates (ξ,η) by

$$z = c \sinh \xi/(\cosh \xi - \cos \eta),$$
$$r = c \sin \eta/(\cosh \xi - \cos \eta). \tag{5}$$

Here c is the half-distance between the points identified by $\xi \to +\infty$ and $\xi \to -\infty$, and the origin is placed midway between these two points. In terms of the radii R_1, R_2 and the distance D between the spheres' centers, the length c is given by

$$c = \frac{D}{2}\left[\left(1 - \frac{R_1^2 + R_2}{D}\right)^2 - 4\frac{R_1^2 R_2}{D}\right]^{1/2}. \tag{6}$$

We note for future reference that the points with coordinates $z = \pm c$ are the images of the foci $\xi \to \pm\infty$ in the spheres.

The sphere 1 in Fig. 1 is defined by $\xi = \beta$ and the sphere 2 by $\xi = -\alpha$. The distance between the spheres' centers is given by

$$D = c(\coth \beta + \coth \alpha), \tag{7}$$

while the spheres' radii are given by

$$R_1 = c/\sinh \beta, \quad R_2 = c/\sinh \alpha. \tag{8}$$

From these relations it is easy to prove that

$$\beta = \cosh^{-1}[(D^2 + R_1^2 - R_2)/2DR_1], \tag{9}$$

$$\alpha = \cosh^{-1}[(D^2 - R_1^2 + R_2)/2DR_2]. \tag{10}$$

The geometry of the problem is completely determined by two dimensionless lengths, which we take to be

$$s = R_2/R_1, \quad d = (D - R_1 - R_2)/R_1. \tag{11}$$

The continuity equation is identically satisfied by the introduction of the Stokes streamfunction $\psi(\xi,\eta)$, related to the velocity components by

$$[u_\xi, u_\eta] = \frac{(\cosh \xi - \cos \eta)^2}{c^2 \sin \eta}\left(\frac{\partial \psi}{\partial \eta}, -\frac{\partial \psi}{\partial \xi}\right). \tag{12}$$

Upon substituting these relations in the curl of the momentum equation we obtain

$$L^2_{-1}(\psi) = 0, \tag{13}$$

where L_{-1} is the axisymmetric Stokes operator in the bipolar coordinate system,

$$L_{-1} = \frac{\sin \eta(\cosh \xi - \cos \eta)}{c^2}\left[\frac{\partial}{\partial \xi}\left(\frac{\cosh \xi - \cos \eta}{\sin \eta}\right)\frac{\partial}{\partial \xi} + \frac{\partial}{\partial \eta}\left(\frac{\cosh \xi - \cos \eta}{\sin \eta}\right)\frac{\partial}{\partial \eta}\right].$$

In terms of the streamfunction the vanishing of the tangential velocity on the particles is expressed by

$$\left.\frac{\partial \psi}{\partial \xi}\right|_{\xi=\beta} = 0, \quad \left.\frac{\partial \psi}{\partial \xi}\right|_{\xi=-\alpha} = 0. \tag{14}$$

The condition of a prescribed normal velocity on sphere 1 leads to

$$\left.\frac{\partial\psi}{\partial\eta}\right|_{\xi=\beta} = V_1 c^2 \frac{\sin\eta}{(\cosh\beta-\cos\eta)^2},$$

with a similar equation for sphere 2. These relations can be integrated with respect to η, which simplifies the calculation. One finds

$$\psi|_{\xi=\beta} = -c^2 V_1/(\cosh\beta-\cos\eta) + c^2 B' \tag{15}$$

and

$$\psi|_{\xi=-\alpha} = -c^2 V_2/(\cosh\alpha-\cos\eta) + c^2 A', \tag{16}$$

where A' and B' are integration constants to be determined.

The general solution to the Stokes equation (13) in bipolar coordinates has been given in Ref. 1 and recently generalized to cases involving sources and sinks in Ref. 13 in the following form:

$$\psi(\xi,\eta) = (\cosh\xi-\cos\eta)^{-3/2} \times \sum_{i=-1}^{\infty} \Xi_n(\xi) C_{n+1}^{-1/2}(\cos\eta), \tag{17}$$

where

$$\Xi_{-1}(\xi) = A(\cosh\tfrac{3}{2}\xi + 3\cosh\tfrac{1}{2}\xi) + B(\sinh\tfrac{3}{2}\xi - 3\sinh\tfrac{1}{2}\xi),$$

$$\Xi_0(\xi) = A(\cosh\tfrac{3}{2}\xi + 3\cosh\tfrac{1}{2}\xi) - B(\sinh\tfrac{3}{2}\xi - 3\sinh\tfrac{1}{2}\xi),$$

and

$$\Xi_n(\xi) = A_n\cosh(n-\tfrac{1}{2})\xi + B_n\sinh(n-\tfrac{1}{2})\xi + C_n\cosh(n+\tfrac{3}{2})\xi + D_n\sinh(n+\tfrac{3}{2})\xi,$$

for $n = 1,2,\ldots$. Here A, B, A_n, B_n, C_n, and D_n are integration constants and $C_{n+1}^{-1/2}$ is the Gegenbauer polynomial of order $(n+1)$ and degree $-\frac{1}{2}$. It may be noted that the general solution used by Sen and Law[19] is incorrect because the source terms are not treated separately. As a consequence, their drag force calculation is also wrong.

In the present problem some simplification is obtained by using the linearity of the Stokes flow to decompose the streamfunction,

$$\psi = c^2 V_1\psi_1 + c^2 V_2\psi_2. \tag{18}$$

Because of the following relation between ψ_1 and ψ_2,

$$\psi_2(\alpha,\beta;\xi,\eta) = \psi_1(\beta,\alpha;\xi,\eta), \tag{19}$$

we only need to solve for one of the streamfunctions, say ψ_1. Accordingly, in the following, we set $V_2 = 0$ and $V_1 = 1$ in the boundary conditions (15) and (16).

The integration constants A' and B' can be calculated by imposing (15) and (16) at the points $\eta = 0,\pi$ on each sphere. A direct substitution yields

$$2\sqrt{2}A = -1/(\cosh\beta+1) + B' = A', \tag{20}$$

$$2\sqrt{2}B = -1/(\cosh\beta-1) + B' = -A', \tag{21}$$

from which

$$A' = 1/(\sinh^2\beta), \quad B' = \cosh\beta/\sinh^2\beta, \tag{22}$$

$$A = (\sqrt{2}/4)(1/\sinh^2\beta), \quad B = -(\sqrt{2}/4)(1/\sinh^2\beta). \tag{23}$$

Next we expand the boundary-condition equations (14)–(16) in series of $C_{n+1}^{-1/2}$. Matching each term in the series arising from (15) and (16) gives the following conditions for Ξ_n:

$$\Xi_n(\beta) = -\frac{1}{\sqrt{2}}e^{-(n+1/2)\beta} - \frac{3B'}{4\sqrt{2}}\left(\frac{e^{-(n-1/2)\beta}}{n-\frac{1}{2}} - \frac{e^{-(n+3/2)\beta}}{n+\frac{3}{2}}\right), \tag{24}$$

$$\Xi_n(-\alpha) = -\frac{3A'}{4\sqrt{2}}\left(\frac{e^{-(n-1/2)\alpha}}{n-\frac{1}{2}} - \frac{e^{-(n+3/2)\alpha}}{n+\frac{3}{2}}\right), \tag{25}$$

while from (14) we have

$$\frac{d\Xi_n}{d\xi}(\beta) = \frac{3(n+\frac{1}{2})}{\sqrt{2}}e^{-(n+1/2)\beta} + \frac{3B'\sinh\beta}{2\sqrt{2}}e^{-(n+1/2)\beta}, \tag{26}$$

$$\frac{d\Xi_n}{d\xi}(-\alpha) = -\frac{3A'\sinh\alpha}{2\sqrt{2}}e^{-(n+1/2)\alpha}. \tag{27}$$

The following special form of $\Xi_n(\xi)$ for $n \geqslant 1$ satisfies the conditions (24) and (25):

$$\Xi_n(\xi) = A_n\frac{\sinh(n-\frac{1}{2})(\beta-\xi)}{\sinh(n-\frac{1}{2})(\beta+\alpha)} + B_n\frac{\sinh(n-\frac{1}{2})(\xi+\alpha)}{\sinh(n-\frac{1}{2})(\beta+\alpha)} + C_n\left(\frac{\sinh(n-\frac{1}{2})(\beta-\xi)}{\sinh(n-\frac{1}{2})(\beta+\alpha)} - \frac{\sinh(n+\frac{3}{2})(\beta-\xi)}{\sinh(n+\frac{3}{2})(\beta+\alpha)}\right) + D_n\left(\frac{\sinh(n-\frac{1}{2})(\xi+\alpha)}{\sinh(n-\frac{1}{2})(\beta+\alpha)} - \frac{\sinh(n+\frac{3}{2})(\xi+\alpha)}{\sinh(n+\frac{3}{2})(\beta+\alpha)}\right), \tag{28}$$

provided that

$$A_n = -\frac{3A'}{4\sqrt{2}}\left(\frac{e^{-(n-1/2)\alpha}}{n-\frac{1}{2}} - \frac{e^{-(n+3/2)\alpha}}{n+\frac{3}{2}}\right), \tag{29}$$

$$B_n = -\frac{1}{\sqrt{2}}e^{-(n+1/2)\beta} - \frac{3B'}{4\sqrt{2}}\left(\frac{e^{-(n-1/2)\beta}}{n-\frac{1}{2}} - \frac{e^{-(n+3/2)\beta}}{n+\frac{3}{2}}\right). \tag{30}$$

We now calculate C_n and D_n by satisfying Eqs. (26) and (27),

$$C_n = (f_n h_n - g_n e_n)/(f_n^2 - g_n^2), \quad D_n = (g_n h_n - f_n e_n)/(f_n^2 - g_n^2), \tag{31}$$

where

$$f_n = (n-\tfrac{1}{2})/\tanh(n-\tfrac{1}{2})(\beta+\alpha) - (n+\tfrac{3}{2})/\tanh(n+\tfrac{3}{2})(\beta+\alpha),$$

$$g_n = (n-\tfrac{1}{2})/\sinh(n-\tfrac{1}{2})(\beta+\alpha) - (n+\tfrac{3}{2})/\sinh(n+\tfrac{3}{2})(\beta+\alpha),$$

$$e_n = \left(n-\frac{1}{2}\right)\left(\frac{B_n}{\tanh(n-\frac{1}{2})(\beta+\alpha)}\right. \tag{32}$$

$$-\frac{A_n}{\sinh(n-\frac{1}{2})(\beta+\alpha)}\Bigg)$$
$$-\frac{3(n+\frac{1}{2})}{\sqrt{2}}e^{-(n+1/2)\beta}-\frac{3B'\sinh\beta}{2\sqrt{2}}e^{-(n+1/2)\beta},$$

$$h_n=\left(n-\frac{1}{2}\right)\left(\frac{B_n}{\sinh(n-\frac{1}{2})(\beta+\alpha)}\right.$$
$$-\frac{A_n}{\tanh(n-\frac{1}{2})(\beta+\alpha)}\Bigg)$$
$$+\frac{3A'\sinh\alpha}{2\sqrt{2}}e^{-(n+1/2)\alpha}.$$

As will be shown in the next section, these expressions contain a number of interesting limit cases. In particular, the limit $\beta\to 0$ corresponds to a sphere in the presence of an evaporating plane wall. Although this limit case is in principle contained in (17), its actual calculation is nontrivial because of the need to identify infinite constants that cancel. For this case it is easier to solve the problem directly to find

$$\psi(\xi,\eta)=(\cosh\xi-\cosh\eta)^{-3/2}\times\sum_{i=1}^{\infty}\Xi_n(\xi)C_{n+1}^{-1/2}(\cos\eta),\tag{33}$$

where

$$\Xi_n(\xi)=B_n\frac{\sinh(n-\frac{1}{2})(\xi+\alpha)}{\sinh(n-\frac{1}{2})\alpha}$$
$$-C_n\left(\frac{\sinh(n-\frac{1}{2})\xi}{\sinh(n-\frac{1}{2})\alpha}-\frac{\sinh(n+\frac{3}{2})\xi}{\sinh(n+\frac{3}{2})\alpha}\right)$$
$$+D_n\left(\frac{\sinh(n-\frac{1}{2})(\xi+\alpha)}{\sinh(n-\frac{1}{2})\alpha}\right.$$
$$\left.-\frac{\sinh(n+\frac{3}{2})(\xi+\alpha)}{\sinh(n+\frac{3}{2})\alpha}\right).\tag{34}$$

Here

$$B_n=(1/\sqrt{2})\left[n(n+1)/(n-\tfrac{1}{2})/(n+\tfrac{3}{2})\right],\tag{35}$$

$$C_n=(f_nh_n-g_ne_n)/(f_n^2-g_n^2),$$
$$D_n=(g_nh_n-f_ne_n)/(f_n^2-g_n^2),\tag{36}$$

$$e_n=(n-\tfrac{1}{2})B_n/\tanh(n-\tfrac{1}{2})\alpha,$$
$$h_n=(n-\tfrac{1}{2})B_n/\sinh(n-\tfrac{1}{2})\alpha.\tag{37}$$

It is easy to see that this system can be reduced by a simple kinematic transformation to that of a sphere approaching a plane with the evaporation velocity V_1. This problem has been solved by Brenner[10] and Maude.[11]

Although exact, the solutions obtained are unfortunately rather complicated. In order to get some insight into the physical processes that they describe it is useful to consider some limiting cases and to show explicitly the streamlines of the flow. This is the object of the next sections.

III. LIMIT CASES

The first limit case we consider is that in which the evaporating sphere collapses to a point. As is clear from (8), the limit $R_1\to 0$ can be obtained by letting β become larger and larger. This situation corresponds to a source in the presence of a sphere. The strength M of the source is

$$M=4\pi R_1^2V_1,$$

or, in terms of β,

$$M=4\pi c^2V_1/\sinh^2\beta,\tag{38}$$

which shows that, as $\beta\to\infty$, V_1 must also tend to infinity in such a way as to keep M constant. It can be shown from (8) and (11) that the source's position takes on the coordinates $r\to 0, z=c$ in the limit.

As $\beta\to\infty$ the leading-order terms in the general solution previously given diverge like $\sinh^{-2}\beta$ and therefore remain finite if this solution is expressed in terms of the source strength M. Indeed, it is clear from (38) that to effect this limit operation the integration constants A', B', A, and B must be multiplied by the factor $\sinh^2\beta/4\pi$. The remaining integration constants A_n, B_n, C_n, and D_n are all proportional to A' and B'. If we combine the terms that are proportional to B' and take the limit $\beta\to\infty$, we obtain three nonzero terms in the series, namely,

$$(\sqrt{2}M/16\pi)\left[(e^{-(3/2)\xi}+3e^{(1/2)\xi})-(e^{(3/2)\xi}\right.$$
$$\left.+3e^{-(1/2)\xi})\cos\eta-2e^{(1/2)\xi}(1-\cos^2\eta)\right].\tag{39}$$

Upon division by the factor $(\cosh\xi-\cos\eta)^{3/2}$ appearing in (17), this result gives

$$(\sqrt{2}M/8\pi)(\cosh\xi-\cos\eta)^{-1/2}(e^{-(1/2)\xi}-\cos\eta e^{(1/2)\xi}),\tag{40}$$

which is readily seen to be just the streamfunction of a point source expressed in bispherical coordinates. It may also be shown that in this limit the expression (28) for Ξ_n becomes

$$\Xi_n=A_ne^{-(n-1/2)(\xi+\alpha)}+C_n(e^{-(n-1/2)(\xi+\alpha)}$$
$$-e^{-(n+3/2)(\xi+\alpha)}),\tag{41}$$

where, from (30) and (32),

$$A_n=\frac{3M}{16\pi\sqrt{2}}\left(\frac{e^{-(n+3/2)\alpha}}{n+\frac{3}{2}}-\frac{e^{-(n-1/2)\alpha}}{(n-\frac{1}{2})}\right)$$
$$C_n=(3M/16\pi\sqrt{2})\left[e^{-(n+3/2)\alpha}-e^{-(n-1/2)\alpha}\right.$$
$$\left.-e^{-(n+3/2)\alpha}/n+\tfrac{3}{2})\right].$$

By suitably combining terms, the series can be summed to obtain the following closed-form expression:

$$\psi = (\sqrt{2}M/8\pi)(\cosh\xi - \cos\eta)^{-3/2}\{\cosh\xi - \cos\eta)(e^{-(1/2)\xi} - \cos\eta e^{(1/2)\xi})$$
$$+ [\cosh(\xi + 2\alpha) - \cos\eta)](\cos\eta\, e^{-1/2(\xi+2\alpha)} - e^{1/2(\xi+2\alpha)})$$
$$+ e^{-2\alpha}e^{-(3/2)\xi}\sinh(\xi+\alpha)(1-\cos^2\eta) + \sqrt{2}[\cosh(\xi+2\alpha) - \cos\eta]^{3/2}$$
$$- 3\sqrt{2}\sinh\alpha\sinh(\xi+\alpha)[\cosh(\xi+2\alpha) - \cos\eta]^{1/2}$$
$$- 3\sinh\alpha\sinh(\xi+\alpha)(\cos\eta e^{(1/2)(\xi+2\alpha)} - e^{-(1/2)(\xi+2\alpha)})\}. \tag{42}$$

This representation of the solution can be rendered more transparent by introducing a spherical coordinate system (R,θ) with the origin placed at the center of the remaining sphere (sphere 2, corresponding to $\xi = -\alpha$) and the radial coordinate scaled by R_2. The image of the source in this sphere is at the point $\xi = -\infty$ and the distance ρ_2 of the generic field point from this image is given by

$$\rho_2 = (R_2/h)(h^2R^2 - 2hR\cos\theta + 1)^{1/2}$$
$$= \sqrt{2}[ce^{(1/2)\xi}/(\cosh\xi - \cos\eta)^{1/2}], \tag{43}$$

where

$$h = D/R_2 = e^{\alpha}. \tag{44}$$

Similarly, the distance ρ_1 from the source is given by

$$\rho_1 = R_2(R^2 - 2hR\cos\theta + h^2)^{1/2}$$
$$= \sqrt{2}[ce^{-(1/2)\xi}/(\cosh\xi - \cos\eta)^{1/2}]. \tag{45}$$

In terms of R, θ, ρ_1, and ρ_2, the expression (42) of the streamfunction simplifies to

$$\psi = \frac{M}{4\pi}\left(R_2\frac{h - R\cos\theta}{\rho_1} + R_2R^2\frac{R\cos\theta - hR^2}{h\rho_2}\right.$$
$$+ R_2^3\frac{R^2-1}{h^2\rho_2^3}R^2\sin^2\theta$$
$$+ R^3 - \frac{3}{2}(R^2-1)R - \frac{3}{2}R_2(R^2-1)$$
$$\left.\times\frac{R\cos\theta - hR^2}{h\rho_2}\right), \tag{46}$$

and coincides with the form given by Collins[8,9] and Hasimoto.[7] By taking the sphere larger and larger (i.e., $h\to 0$) we find the solution for the flow induced by a point source near a wall, as in Blake and Chwang,[20] who used Lorentz's reflection principle

$$\psi = \frac{M}{4\pi}\left(\frac{H-z}{\rho_1} - \frac{H+z}{\rho_2} + 4\frac{zr^2}{\rho_2^3}\right). \tag{47}$$

Here H is the distance of the source from the wall and r and z are dimensional cylindrical coordinates centered at the point where the normal to the wall passing through the source meets the wall. Now the distances ρ_1 and ρ_2 of the generic field point from the source and its image in the wall are given by

$$\rho_1 = [r^2 + (z-H)^2]^{1/2}, \quad \rho_2 = [r^2 + (z+H)^2]^{1/2}. \tag{48}$$

Another interesting limit case is that in which the spheres are far apart so that the distance D between their centers is much larger than the radii. In this limit the relation between the radii, R_1, R_2, and D is given by

$$R_1/D \simeq e^{-\beta}, \quad R_2/D \simeq e^{-\alpha}, \tag{49}$$

so that α and β are both large. If we take the general solution (17) and keep only the first four terms the following form of the streamfunction is obtained:

$$\psi_1 \simeq (\cosh\xi - \cos\eta)^{-3/2}A\left\{(e^{-(3/2)\xi} + 3e^{(1/2)\xi} - \cos\eta(e^{(3/2)\xi} + 3e^{-(1/2)\xi}) - 2(1-\cos^2\eta)e^{(1/2)\xi}\right.$$
$$+ \frac{1}{2}(1-\cos^2\eta)\left[\frac{3}{2}e^{-\alpha}e^{-(1/2)\xi} + \left(2e^{-2\beta} - \frac{9}{4}e^{-\alpha}e^{-\beta}\right)e^{1/2\xi} + 2e^{-2\beta}e^{(5/2)\xi}\right]$$
$$\left. + \frac{1}{2}\cos\eta(1-\cos^2\eta)(-4e^{-2\beta})e^{(3/2)\xi}\right\}, \tag{50}$$

where terms of order $e^{-3\beta}$, $e^{-3\alpha}$, etc. have been neglected. By using the above relations and combining certain terms, it is possible to simplify the expression. Thus we find the following approximate result for the streamfunction:

$$\psi \simeq V_1R_1^2\left\{\frac{c-z}{\rho_1} - \frac{1}{2}\left(\frac{r}{D}\right)^2\left[\frac{3}{2}\frac{R_2}{\rho_2}\right.\right.$$
$$\left.\left. - \frac{9}{4}\frac{R_2}{D}\frac{R_1}{\rho_1} + 2\frac{D}{R_1}\left(\frac{R_1}{\rho_1}\right)^3\right]\right\}, \tag{51}$$

where again the cylindrical coordinates (5) have been used, ρ_1 and ρ_2 are given by (45) and (43), and, to a consistent order,

$$c \simeq (D/2)[1 - (R_1^2 + R_2^2)/D^2].$$

A further case of interest, which can be analyzed along similar lines, is that of an evaporating sphere at a large distance from a plane, nonevaporating wall. This limit is obtained for $\alpha\to 0$ in (50). The result is

$$\psi \simeq V_1R_1^2\left\{\left(\frac{c-z}{\rho_1} - \frac{c+z}{\rho_2} + 4\frac{zr^2}{\rho_2^3}\right)\right.$$
$$\left. + \frac{9}{32}\left(\frac{r}{H}\right)^2\frac{R_1}{\rho_2}\left[3 - 2\frac{\rho_2}{\rho_1} - \left(\frac{\rho_2}{\rho_1}\right)^2\right]\right\}. \tag{52}$$

Here H is the distance of the center of the evaporating sphere

(sphere 1) from the wall and $c \simeq H(1 - R_1^2/2D^2)$.

As a final limit case we consider a nonevaporating sphere at a large distance from a plane, evaporating wall. In this case we start from the solution (33) and assume α to be large to find

$$\psi_1 \simeq \frac{1}{2}\frac{\sin^2\eta}{(\cosh\xi - \cos\eta)^2} + \frac{\sqrt{2}}{2}(\cosh\xi - \cos\eta)^{-3/2}\left[e^{(1/2)\xi}\left(3e^{-\alpha} + \frac{27}{4}e^{-2\alpha}\right) - e^{-(1/2)\xi}\left(\frac{9}{2}e^{-\alpha} + \frac{13}{2}e^{-2\alpha}\right) + e^{-(5/2)\xi}\left(\frac{3}{2}e^{-\alpha} + \frac{7}{4}e^{-2\alpha}\right)\right], \tag{53}$$

or, in terms of cylindrical coordinates,

$$\psi \simeq \frac{1}{2}r^2 V_1\left\{1 + \frac{R_2^2}{4H^2}\left[\frac{3R_2}{\rho_1}\left(2 + \frac{9}{4}\frac{R_2}{H}\right) - \frac{R_2}{\rho_2}\left(9 + \frac{13}{2}\frac{R_2}{H}\right) + \frac{R_2}{\rho_2}\left(\frac{\rho_1}{\rho_2}\right)^2\left(3 + \frac{7}{4}\frac{R_2}{H}\right)\right]\right\}. \tag{54}$$

Here H is the distance of the center of the nonevaporating sphere (sphere 2) from the wall and $c \simeq H(1 - R_2^2/2D^2)$.

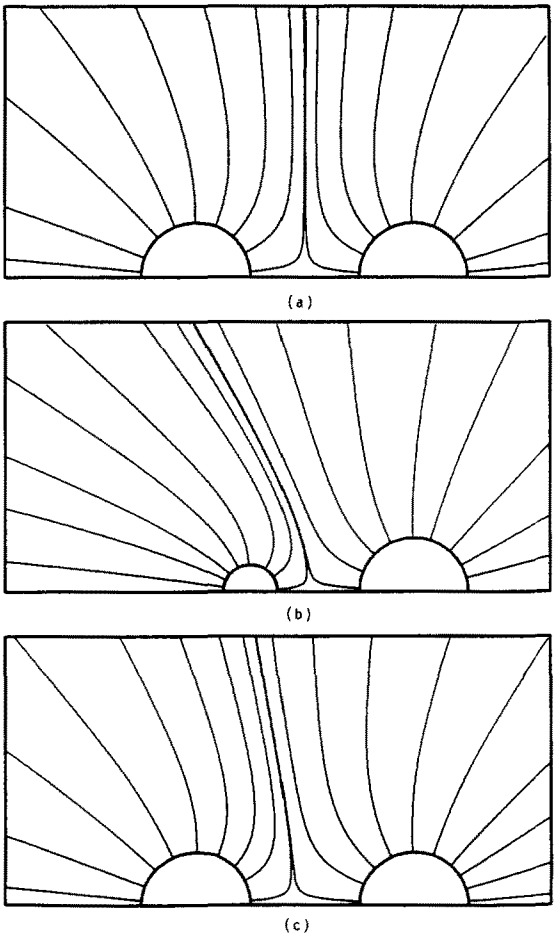

FIG. 2. Streamlines of two evaporating spheres at a dimensionless distance d defined by (11) equal to 2. In (a) the radii and the evaporation velocities are equal. In (b) $R_2/R_1 = 0.5$, again with equal velocities. (c) $R_2 = R_1$ and $V_2/V_1 = 0.5$.

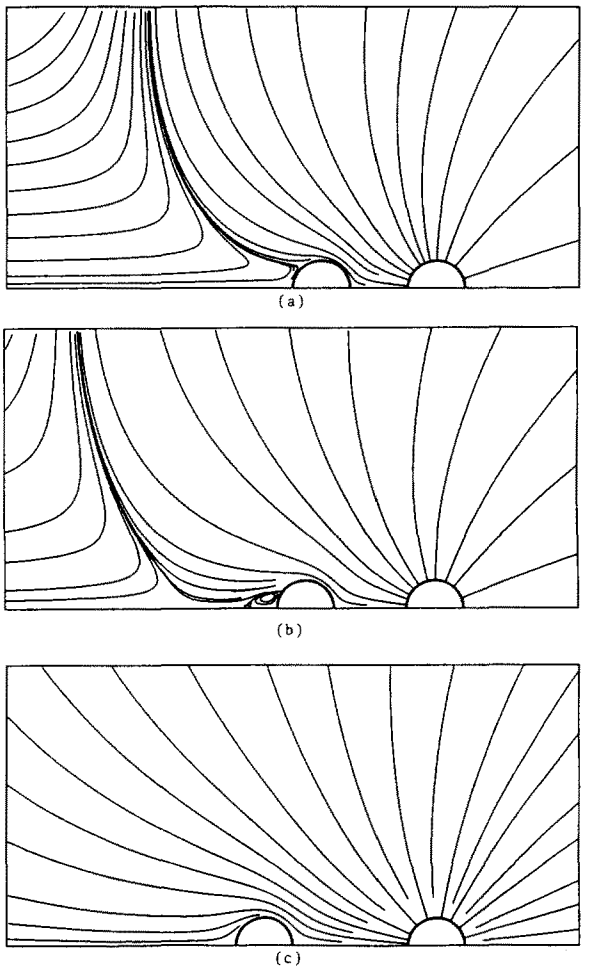

FIG. 3. Streamline plot showing the effect of a varying distance between spheres when only the sphere at the right is evaporating. Here the radii are equal and d is 3, 2.25, and 2 for cases (a), (b), and (c), respectively.

IV. FLOW FIELD

In this, as in many other problems, the pattern of streamlines is particularly revealing and key features of the flow may be missed without its analysis. The streamlines formed by two equal and equally evaporating spheres, which are shown in Fig. 2(a), are not unexpected. The stagnation point is at the midpoint of the segment joining the spheres' centers. It is also found that when the right sphere is made bigger than the left one, still maintaining an equal evaporation rate, the stagnation point moves to the left [Fig. 2(b)]. Predictable changes also occur if the radial velocity ratio is decreased, so that the left sphere evaporates less than the right one [Fig. 2(c)].

These results become more interesting if the individual flows resulting from each sphere are examined separately, which we do in Fig. 3 for spheres of equal radius. Here we set V_2 to zero and consider the flow field produced by the evaporation of sphere 1 alone. In Fig. 3(a) the dimensionless distance d defined in (11) is 3. The streamlines again look predictable. The flow of vapor goes around the second sphere to infinity. But when the distance between the spheres is decreased to $d = 2$ [Fig. 3(c)], we observe the presence of an

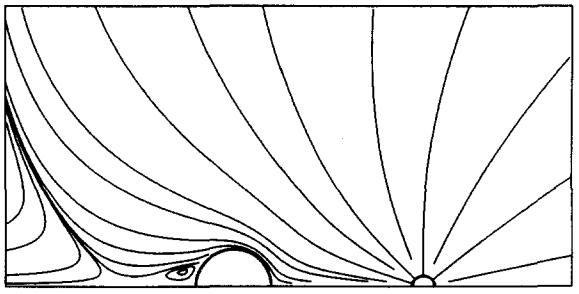

FIG. 4. Flow pattern induced by a point source near a sphere obtained from the closed-form solution (42). Here $(D - R_2)/R_2$ equals 5.

infinite recirculation zone behind the nonevaporating particle. (This zone is actually also present in the previous example of Fig. 3(a) but is out of the frame of the picture.) This is an interesting example of the separation behavior at a smooth boundary, the possible occurrence of which in Stokes flow is well known.[21] Even more interestingly, for distances between the spheres intermediate between those of Figs. 3(a) and 3(c), a closed recirculation zone behind the nonevaporating sphere is found in addition to the infinite one [Fig. 3(b)].

To be sure that the small recirculation is not a numerical artifact, we plot in Fig. 4 the streamlines of the closed-form solution previously given for the case of a point source near a sphere. The small and the infinite eddies are present in this limit case as well. This finding indicates that this behavior is rather insensitive to the radius ratio as long as the evaporating sphere is smaller than the other one. In this case also there is an infinite recirculating region that is pushed farther away behind the nonevaporating sphere as the radius of the evaporating sphere increases.

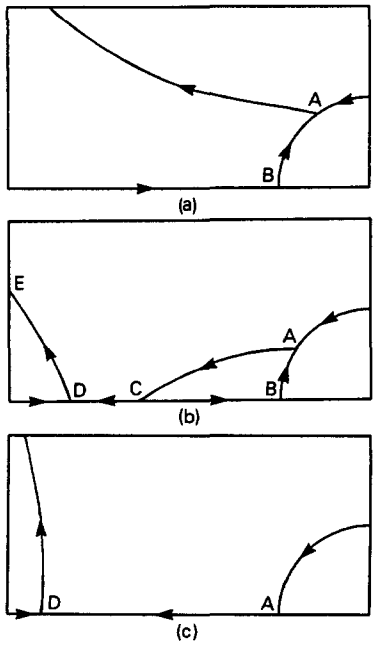

FIG. 5. Detail (not to scale) of the different flow regimes shown in Fig. 3 in the neighborhood of the back of the nonevaporating sphere. The transition from case (a)–(c) occurs as the distance between the spheres is increased.

The change between the regimes of flow shown in Fig. 3 may be described in greater detail with reference to Fig. 5, in which the flow near the back of the nonevaporating sphere is sketched (not to scale). At relatively small distances [Fig. 5(a)] there are a separation point A and a stagnation point B on the sphere. As the distance increases, the streamline issuing from A curves downward and gives rise to the streamline ACDE in Fig. 5(b). This "captures" the small recirculating eddie behind the sphere. As the distance increases further, the points A and C of Fig. 5(b) move closer and closer toward B and the recirculating region disappears [Fig. 5(c)]. At the same time the streamline issuing from the stagnation point D becomes steeper and steeper.

These results indicate that one can classify the flow by looking at the velocity on the axis of symmetry behind the second drop. If the sign of the velocity does not change as one moves away from the sphere, the flow is of the type shown in Fig. 3(a) or 5(a). If the sign changes twice the flow is of the type shown in Fig. 3(b) or 5(b), and if the sign changes only once the flow is of the type shown in Fig. 3(c) or 5(c). These flow regimes are sketched in the parameter space (s,d) in Fig. 6. In this figure, the boundaries are not exact but estimated on the basis of numerical results at discrete points. A noteworthy feature of this diagram is that for radius ratios smaller than about 0.4 the flow separation on the nonevaporating sphere does not occur as the distance between the spheres becomes smaller.

In summary, we can say that the flow has two basic regimes and a transition regime. In the first regime the infinite recirculation zone is detached from the nonevaporating particle. This happens when the particles are far enough from each other. The second regime manifests itself by having the recirculation zone attached to the nonevaporating particle when the gap between the spheres is less than approximately one radius. In the transition zone, a finite recirculation zone behind the nonevaporating particle appears. However, as usually happens in Stokes flow, the fluid in this small recirculation region is nearly stagnant. Therefore, in the full problem in which the effects of the flow field on the phase change process are considered, it can be expected that this feature will have a negligible effect on the heat transfer.

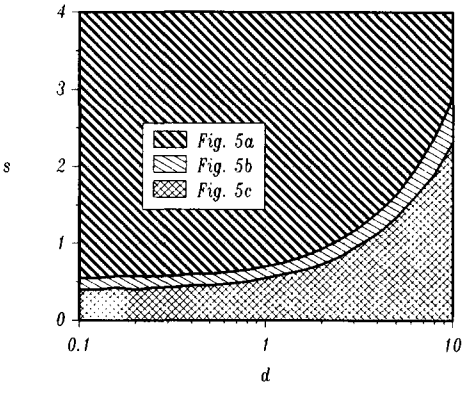

FIG. 6. Diagram in the space of parameters $s = R_2/R_1$, $d = (D - R_1 - R_2)/R_1$, showing the occurrence of the different flow structures shown in Figs. 3 and 5. The boundaries between the regions are not exact, but only an estimate based on numerical results at discrete points.

Results bearing a general resemblance to those found here may be found in Ref. 22 where the Stokes flow induced by various singularities near a caplike obstacle is considered.

V. DRAG

As a result of the linearity of the problem, the total force on each sphere is simply the sum of the forces induced by V_1 and V_2. Therefore, we may write the total forces F_1 and F_2 on spheres 1 and 2, respectively, as

$$F_1 = \pi\mu V_1 R_1 F_{11}(\beta,\alpha) + \pi\mu V_2 R_2 F_{12}(\beta,\alpha) \tag{55}$$

and

$$F_2 = \pi\mu V_1 R_1 F_{21}(\beta,\alpha) + \pi\mu V_2 R_2 F_{22}(\beta,\alpha). \tag{56}$$

This decomposition is reminiscent of the introduction of resistance coefficients in other two-sphere Stokes problems.[6,23]

By using symmetry arguments it is easy to show that the nondimensional force coefficients F_{ij} are related as follows:

$$F_{11}(\beta,\alpha) = -F_{22}(\alpha,\beta), \quad F_{21}(\beta,\alpha) = -F_{12}(\alpha,\beta). \tag{57}$$

It is therefore sufficient to determine F_{11} and F_{21} to have a complete description of the forces between the two spheres. It would be useful to obtain another relation between $F_{12}(\beta,\alpha)$ and $F_{21}(\beta,\alpha)$ by use of the Lorentz reciproal theorem. Actually, this proves to be impossible to do in a simple way because of the net flow of momentum at infinity and to the complexity of the near-field flow.

The drag formula in the bispherical coordinate system was given by Stimson and Jeffery[1] and generalized by Oguz and Sadhal[13] to cases involving sources and sinks. The application of this drag formula to the present case gives

$$F_{11} = 2\sqrt{2}\left[4A - 4B + \sum_{n=1}^{\infty}\left(\frac{(B_n + D_n)e^{(n-1/2)\alpha} - (A_n + C_n)e^{-(n-1/2)\beta}}{\sinh(n-\frac{1}{2})(\alpha+\beta)} - \frac{D_n e^{(n+3/2)\alpha} - C_n e^{-(n+3/2)\beta}}{\sinh(n+\frac{3}{2})(\alpha+\beta)}\right)\right]\sinh\beta, \tag{58}$$

$$F_{21} = 2\sqrt{2}\left[4A + 4B + \sum_{n=1}^{\infty}\left(-\frac{(B_n + D_n)e^{-(n-1/2)\alpha} - (A_n + C_n)e^{-(n-1/2)\beta}}{\sinh(n-\frac{1}{2})(\alpha+\beta)} + \frac{D_n e^{-(n+3/2)\alpha} - C_n e^{(n+3/2)\beta}}{\sinh(n+\frac{3}{2})(\alpha+\beta)}\right)\right]\sinh\beta. \tag{59}$$

In Figs. 7 and 8 the force coefficients $F_{11}(\beta,\alpha)$ and $F_{21}(\beta,\alpha)$ are plotted against the dimensionless distance d defined by (11) for various radius ratios. The forces cover a wide range of values but, in general, exhibit two distinct regimes. When the two particles are close (i.e., d is small) the drag force varies linearly with respect to $1/d$ (note that the scale is logarithmic and therefore the slope is -1). Upon effecting a simple kinematic transformation, it is seen that this limiting case closely resembles that in which two nonevaporating spheres approach each other. In this situation, if the gap between the spheres is small compared to their radii, a modified lubrication approximation can be used to calculate the drag as shown by Jeffrey.[5] To leading order he found F_{11} and F_{21} to be

$$F_{11} \simeq F_{21} \simeq 6/(1 - R_1/R_2)^2 d. \tag{60}$$

In Figs. 9(a) and 9(b), we plot the coefficients given by (58) and (59) multiplied by $(1 - R_1/R_2)^2 d$. For small values of d, according to the approximation (60), the result should be the constant 6. This is indeed confirmed by the figures over a

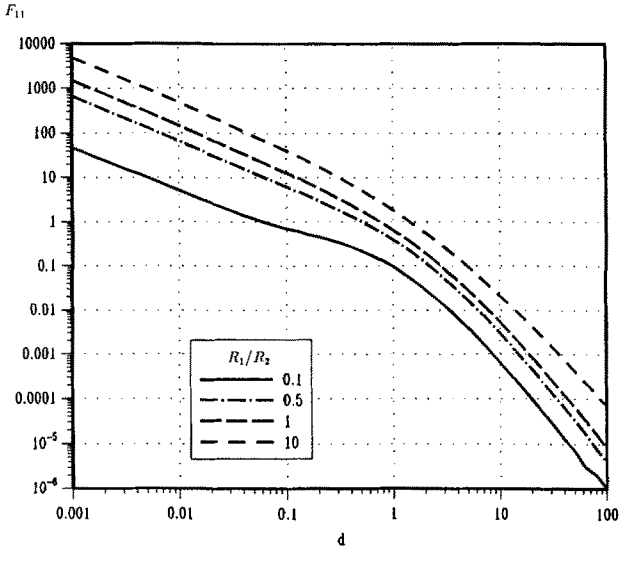

FIG. 7. The "self" force coefficient F_{11} defined by (58) as a function of the dimensionless distance between the spheres $d = (D - R_1 - R_2)/R_2$ for different values of the ratio R_2/R_1.

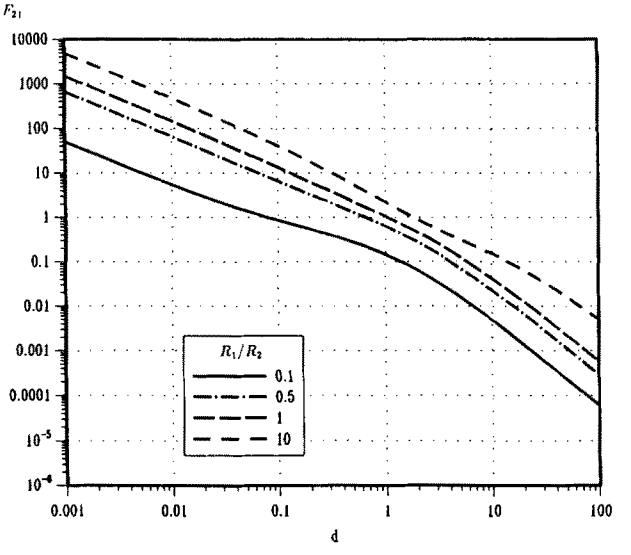

FIG. 8. The "induced" force coefficient F_{21} defined by (59) as a function of the dimensionless distance between the spheres $d = (D - R_1 - R_2)/R_2$ for different values of the ratio R_2/R_1.

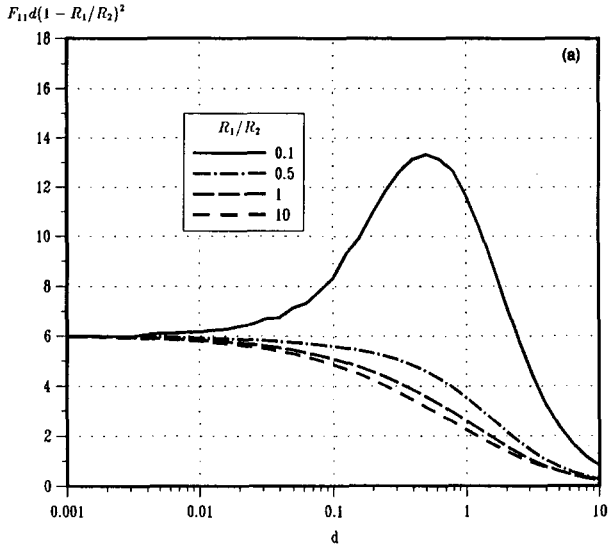

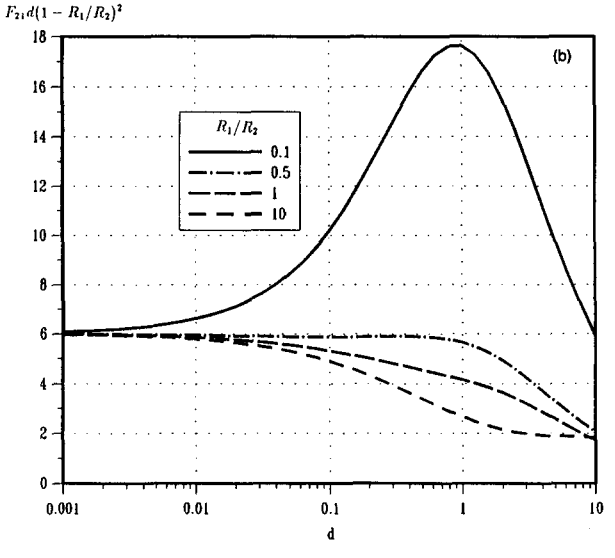

FIG. 9. Plots of (a) F_{11} and (b) F_{21}, scaled by the asymptotic value (60) for small d, i.e., closely spaced spheres. In both cases departure from the constant value 6 indicates the limit of validity of the approximate result (60). The slight irregularity in (a) is a numerical artifact.

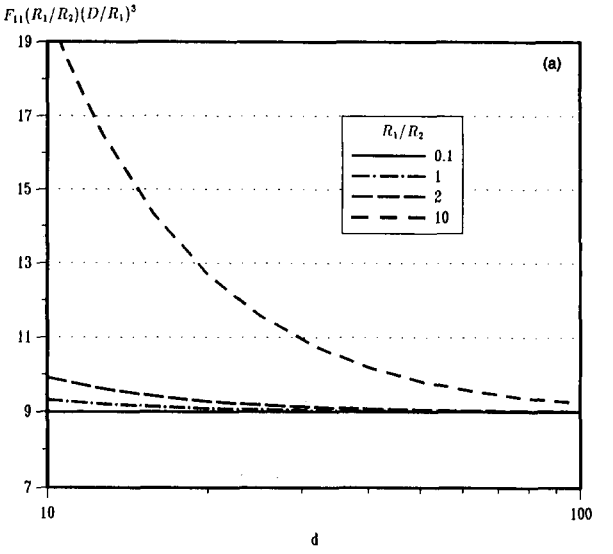

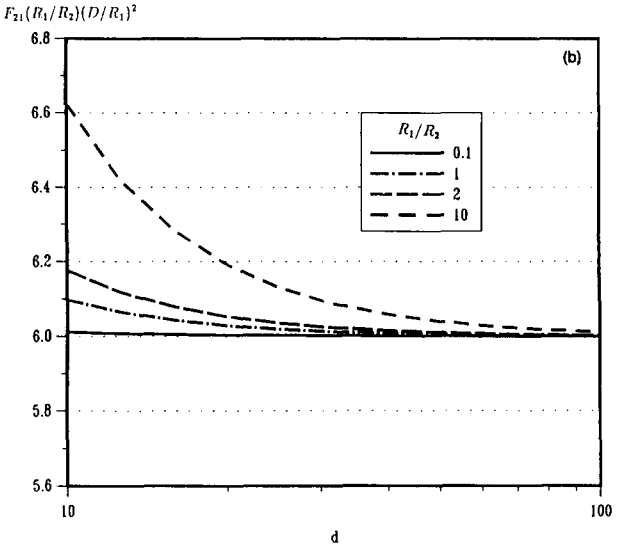

FIG. 10. Plots of (a) F_{11} and (b) F_{21}, scaled by the asymptotic values (61) and (62) for large d, i.e., widely spaced spheres. Departure from the constant values 9 and 6, respectively, indicates the limit of validity of the approximation.

greater and greater range of values of d, as the evaporating sphere (sphere 1) becomes smaller than the other one. This shows that the flow outside the gap region contributes very little to the drag.

The other limit is when the distance between the spheres is large. From Figs. 7 and 8 we see that F_{11} and F_{21} decay like $1/d^3$ and $1/d^2$, respectively. The asymptotic form of these force coefficients can be obtained by an asymptotic analysis of our expressions (58) and (59) or, more simply, by the method reflections. The results are

$$F_{11} \simeq 9(R_2/R_1)(R_1/D)^3 \tag{61}$$

and

$$F_{21} \simeq 6(R_2/R_1)(R_1/D)^2. \tag{62}$$

It is readily recognized that the result for F_{21} can be obtained from the standard formula of Stokes' drag using the flow velocity $V_1 R_1^2/D^2$ induced by the evaporation of sphere 1 at the position of sphere 2. It may be noted that, to lowest order, the term arising from Faxen's law vanishes because the Laplacian of the velocity field, due to a source, is zero. This circumstance increases the domain of validity of these approximate expressions. It is also apparent from these results, and can be verified on the general formulas, that the forces between the particles do not satisfy the action–reaction principle, which indicates a net flow of momentum to infinity. This is associated with the open recirculating eddy that was described in the previous section.

A close examination of Figs. 7 and 8 reveals that transition between the different flow regimes shown in Figs. 5 or 6 does not have, *per se*, a large effect on the interparticle forces.

We can also compare the asymptotic value (62) of F_{21} to drag induced by a point source. By applying the same drag

formula (59) and summing the series, we arrive at the following simple expression for the drag exerted on a nonevaporating sphere by a source of strength M:

$$F_2 = \frac{3}{2}\mu \frac{M}{R_2} \frac{(R_2/D)^3 - (R_2/D)}{(D/R_2) - (R_2/D)}. \tag{63}$$

This result is to be compared with F_2 in (56) written, instead that in terms of the evaporating velocity V_1, in terms of the source strength $M = 4\pi R_1^2 V_1$,

$$F_2 = \frac{3}{2}\mu \frac{M}{R_2}\left(\frac{R_2}{D}\right)^2. \tag{64}$$

Evidently, the two expressions coincide to leading order. It is obvious that the force on the source F_1 is zero. Figure 10(a) is a plot of the force coefficient F_{11} multiplied by $(R_1/R_2)(D/R_1)^3$. The approximate result (61), which should apply when the spheres are far away, is indeed seen to hold to a greater and greater accuracy as R_1 gets smaller. The approximation holds very well for any radius ratio as long as the distance between the two spheres is larger than R_1. This is expected, because in the absence of the sphere 2, the flow would be completely described by a source located at the center of sphere 1. In Fig. 10(b) we show F_{21} multiplied by the same factor, which should equal 6, according to (62). A similar conclusion holds. Since in practical situations dominated by pairwise (as opposed to higher-order) interactions the average distance between the particles will be larger than the radius, it is expected that the above formulas would be useful in many such cases.

In conclusion we show the approximate expressions valid for a sphere at a large distance from a plane. If the sphere is evaporating and the plane is not, we have from (52)

$$F_{11} \simeq 18(R_1/D)^2.$$

In the converse case of a nonevaporating sphere in the presence of an evaporating plane we have from (33)

$$F_{21} = 2\sqrt{2}\left[\sum_{n=1}^{\infty}\left(-\frac{(B_n + D_n)e^{-(n-1/2)\alpha} - C_n}{\sinh(n-1/2)\alpha} + \frac{D_n e^{-(n+3/2)\alpha} - C_n}{\sinh(n+3/2)\alpha}\right)\right]\sinh\alpha, \tag{65}$$

and, when the sphere is far from the plane,

$$F_{21} \simeq 6(1 + \tfrac{9}{8}R_2/D).$$

These last two results have been previously given by Brenner[10] and Maude[11] for the closely related problem of a sphere moving toward a plane.

ACKNOWLEDGMENTS

The authors wish to thank the referees and Dr. John Blake, Dr. Allen T. Chwang, and Dr. Ashok Sangani for some useful comments.

The initial portion of this study was supported by the Ministero della Pubblica Istruzione of Italy. Most of the work was, however, supported by the National Science Foundation Grant No. MSM-8607732.

[1] M. Stimson and G. B. Jeffery, Proc. R. Soc. London Ser. A **111**, 110 (1926).
[2] A. J. Goldman, R. G. Cox, and H. Brenner, Comput. Eng. Sci. **21**, 1151 (1966).
[3] C. J. Lin, K. J. Lee, and N. F. Sather, J. Fluid Mech. **43**, 35 (1970).
[4] E. Rushton and G. A. Davies, Int. J. Multiphase Flow **4**, 357 (1973).
[5] D. J. Jeffrey, Mathematika **29**, 58 (1982).
[6] D. J. Jeffrey and Y. Onishi, J. Fluid Mech. **139**, 261 (1984).
[7] H. Hasimoto, J. Phys. Soc. Jpn. **11**, 793 (1956).
[8] W. D. Collins, Mathematika **1**, 125 (1954).
[9] W. D. Collins, Mathematika **5**, 118 (1958).
[10] H. Brenner, Chem. Eng. Sci. **16**, 242 (1961).
[11] A. D. Maude, Br. J. Appl. Phys. **12**, 293 (1961).
[12] G. K. Batchelor, J. Fluid Mech. **52**, 245 (1972).
[13] H. N. Oguz and S. S. Sadhal, J. Fluid Mech. **179**, 105 (1987).
[14] M. E. O'Neill, Mathematika **11**, 67 (1964).
[15] S. L. Goren and M. E. O'Neill, Chem. Eng. Sci. **26**, 325 (1971).
[16] S. Haber, G. Hetsroni, and A. Solan, Int. J. Multiphase Flow **1**, 57 (1973).
[17] E. Rushton and G. A. Davies, Int. J. Multiphase Flow **9**, 337 (1978).
[18] M. Meyyapan, W. R. Wilcox, and R. S. Subramanian, J. Colloid Interface Sci. **83**, 199 (1981).
[19] A. K. Sen and C. K. Law, Int. J. Heat Mass Transfer **27**, 1418 (1984).
[20] J. R. Blake and A. T. Chwang, J. Eng. Math. **8**, 23 (1974).
[21] H. Hasimoto and O. Sano, Annu. Rev. Fluid Mech. **12**, 335 (1980).
[22] C. Sozou, J. Appl. Math. Phys. **35**, 642 (1984).
[23] S. Kim and R. T. Mifflin, Phys. Fluids **28**, 2033 (1985).